Heliyon 10 (2024) e27942

Contents lists available at ScienceDirect

Heliyon

journal homepage: www.cell.com/heliyon

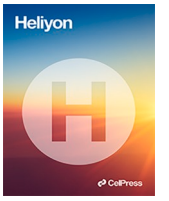

Research article

Pathological and imaging features, treatment, and prognosis of primary intraventricular lymphoma: A review of cases from a single center

Yuqiao Wang [a,1], Chengcheng Cui [a,1], Hafiz Khuram Raza [b,1], Hao Chen [a], Xiangbu Wang [c], Wei Zhang [a], Wenqing Meng [a], Keke Li [d], Zhifeng Mao [e,f,**], Xiujuan Sun [g,***], Shenyang Zhang [a,*]

[a] Department of Neurology, The Affiliated Hospital of Xuzhou Medical University, Xuzhou, China
[b] Academician Expert Workstation of Fengxian District, Shanghai Yuansong Biotechnology Limited Company, Shanghai, China
[c] Department of Pathology, The Affiliated Hospital of Xuzhou Medical University, Xuzhou, China
[d] Department of Radiology, The Affiliated Hospital of Xuzhou Medical University, Xuzhou, China
[e] Neuroimmunology Group, KingMed Diagnostic Laboratory, Guangzhou, China
[f] Department of Clinical Medicine, Medical School, Xiangnan University, Chenzhou, China
[g] Department of Neurology, Liaocheng People's Hospital, China

ARTICLE INFO

Keywords:
Primary intraventricular lymphomas
Clinical features
Imaging characteristics
Diagnosis
Treatment
Prognosis

ABSTRACT

Purpose: The purpose of this retrospective study was to analyze the imaging and pathological features, treatment, and prognosis of patients with primary intraventricular lymphomas (PIL) in order to enhance physicians' understanding of the diagnosis and treatment of PIL.

Methods: A retrospective analysis was conducted on 13 cases of PIL that were hospitalized in our institution. Clinical and imaging data of the patients were collected and compared with the pathology data to summarize and analyze the qualitative diagnostic value of magnetic resonance (MR) features.

Results: Among the enrolled patients, there were nine males and four females, with an average age of (56 ± 9.0) years. The major clinical features observed in PIL patients were headache and dizziness. All 13 patients underwent plain and contrast-enhanced MR scans, revealing multiple foci in 7 cases and single foci in 6 cases. The lesions were located in the lateral ventricle in 10 cases, the third ventricle in 4 cases, and the fourth ventricle in 4 cases. Plain MR scans demonstrated an isointense or slightly hypointense signal on T1-weighted imaging (T1WI) and an isointense or slightly hyperintense signal on T2-weighted imaging (T2WI). Contrast-enhanced scans showed uniform and consistent enhancement of the tumors. Surgical treatment was performed in all patients, and postoperative pathology confirmed the presence of diffuse large B-cell lymphoma.

* Corresponding author. Department of Neurology, the Affiliated Hospital of Xuzhou Medical University, Huaihai West Road, Xuzhou, China.
** Corresponding author. Department of Pathology, The Affiliated Hospital of Xuzhou Medical University, Xuzhou, China
*** Corresponding author. Department of Neurology, the Affiliated Hospital of Xuzhou Medical University, Huaihai West Road, Xuzhou, China.
E-mail addresses: salide111@163.com (X. Sun), zhangshenyang111@163.com (S. Zhang).
[1] Equal contributions: These authors contributed equally to this study.

https://doi.org/10.1016/j.heliyon.2024.e27942
Received 22 December 2023; Received in revised form 7 March 2024; Accepted 8 March 2024
Available online 10 March 2024

Conclusions: PIL exhibits specific imaging and pathological features, with diffuse large B-cell lymphoma being the main pathological type. Pathological examination and immunophenotype analysis serve as the gold standards for PIL diagnosis.

Summary

- Diffuse large B-cell lymphoma is the predominant pathological type in primary intraventricular lymphomas (PIL).
- The specific imaging features of PIL include multiple foci on MR scans, commonly located in the lateral, third, or fourth ventricle.
- Surgical intervention is a common treatment for PIL, and postoperative pathology is crucial for confirming the diagnosis.
- Pathological examination and immunophenotype analysis are emphasized as essential gold standards for accurate PIL diagnosis and understanding its unique features.

1. Introduction

Primary central nervous system lymphoma (PCNSL) is a rare, highly malignant, and aggressive non-Hodgkin lymphoma that primarily affects the central nervous system (CNS). It accounts for approximately 1% of intracranial tumors [1]. The most prevalent pathological type of PCNSL is large B-cell lymphoma [2]. This study focuses explicitly on primary intraventricular lymphoma (PIL), which represents around 4.4%–11.8% of PCNSL cases [3]. While most PCNSLs are located in the brain parenchyma, primary lymphomas in the intraventricular space are uncommon [4]. Since 2000, the overall incidence of PCNSL has increased, particularly among the elderly population. The 5-year and 10-year survival rates for PCNSL are 29.9% and 22.2%, respectively [5]. The prognosis, diagnosis, and treatment of PIL differ from other types of non-Hodgkin lymphoma (NHL). Notably, recent research has shown that PIL is more prevalent in males compared to other PCNSLs [4]. Clinical manifestations of PIL primarily result from increased intracranial pressure and commonly include symptoms such as headache, nausea, and vomiting. Additionally, the obstruction of cerebrospinal fluid flow by the tumor can lead to hydrocephalus. The specific symptoms can vary depending on the affected ventricle. While most PILs present as solitary lesions, there have been instances of multiple lesions, likely due to the spread of tumor cells through cerebrospinal fluid flow. PILs are prone to misdiagnosis, particularly when located in the fourth ventricle, and multiple lesions can be mistaken for metastatic lesions [6]. Therefore, timely and accurate diagnosis is crucial for initiating appropriate treatment and improving clinical outcomes. However, the available data on the diagnosis and treatment of PIL is limited. Diagnosing PIL typically involves neuroimaging such as magnetic resonance imaging (MRI) and cerebrospinal fluid examination for cytologic abnormalities. Histopathological confirmation is essential, although it might be challenging given the location of the lesions within the ventricles [7]. Current treatment recommendations for PCNSL, which apply to PIL, involve a combination of therapies tailored to individual circumstances. Common treatment modalities include radiotherapy, chemotherapy, targeted therapies, and combination approaches [7, 8]. However, it must be noted that the optimal treatment strategy for PIL remains undefined due to the scarcity of dedicated studies. It is, therefore, essential to summarize the clinical symptoms and imaging features of PIL to enhance the specificity and sensitivity of its diagnosis. This study aims to describe the clinical and imaging findings observed in our cohort of patients.

2. Methods

Ethical statement

This study was approved by the Ethics Committee of the Affiliated Hospital of Xuzhou Medical University.

2.1. General information

We conducted a retrospective analysis of clinical data from 13 patients with PIL who were hospitalized between January 2015 and August 2022. The diagnoses were confirmed through surgery and pathology. The study cohort consisted of nine males and four females, ages between 39 and 70 years (mean age: 56 $\pm$ 9.0 years). All enrolled patients had complete MR scan data, including both plain and contrast-enhanced scans, and some patients also underwent proton magnetic resonance spectroscopy (1H-MRS).

The inclusion criteria were as follows:

1. Patients who underwent plain and contrast-enhanced MR scans.
2. Patients with a histopathological diagnosis confirmed as large B-cell lymphoma involving the ventricle and periventricle.
3. Patients without immune deficiency or other primary lesions.
4. Patients who had not received treatment for the lesion prior to surgery.
5. Patients with clear image data that did not affect the diagnosis.

The exclusion criteria were as follows:

Table 1
Characteristics of the 13 patients included in the series.

Case No.	Age (yrs)	Sex	ICS	Location	Size (cm)	HD	GP	SOE	Complication	AT	FU (mos), status	Relapse
1	53	M	Headache, dizziness	LV	77*50*35 mm	N	Cluster like	PTR	Lung infection	CMT + RT	60 months died	Y
2	45	F	Headache, dizziness	LV,CC	43*34*35 mm	N	Solitary nodular	GTR	N	CMT + RT	78 months, died	N
3	57	M	Headache, Dizziness, Limb weakness	LV,4th V	–	N	Cluster like	GTR	N	CMT + RT	33 months died	Y
4	56	F	Dizziness	LV	32*25*20 mm	N	Solitary nodular	PTR	N	CMT + RT	6 months, died	Y
5	61	M	Dizziness, Vomiting	4th V	–	Y	Solitary nodular	GTR	N	CMT + RT	35 months, died	N
6	56	F	Dizziness, Vomiting	LV	32*25*20 mm	N	Solitary nodular	GTR	N	–	20 months died	Y
7	58	M	Dizziness, Vomiting, Limb weakness, Memory d ecline	3rd V	18*13*5 mm	Y	Solitary nodular	PTR	N	–	2 months, died	N
8	68	F	Limb weakness, aphasia, Lethargy, Incontinence	LV,CC	–	N	Cluster like	STR	N	–	2 months, died	N
9	70	M	Limb weakness, Lethargy	LV, 3rd V	–	N	Diffuse type	PTR	N	CMT + RT	1 months, died	N
10	64	M	Dizziness, Blurry vision, Epilepsy	LV,Thalamic region	13*16*14 mm	N	Cluster like	PTR	N	–	1.7 months, died	N
11	57	M	Memory loss, Cognitive impairment, Limb weakness	LV, 3rd V, 4th V, CC	–	N	Cluster like	–	N	CMT + ABMSC	23 months, alive	N
12	46	M	Blurry vision, Limb weakness, Dizziness	4th V	–	y	Cluster like	–	N	CMT	10 months, died	N
13	39	M	Headache, Dizziness, Blurry vision	LV, 3rd V	10*10*5 mm	N	Cluster like	GTR	N	CMT	34 months, alive	N

ICS, Initial clinical symptoms; 3rd V, third ventricle; 4th V, fourth ventricle; LV, lateral ventricle; CC, Corpus callosum; HD,hydrocephalus; Y, yes; N, no; GP, Growth Pattern; SOE, Scope Of Excision; GTR, gross total resection; STR, subtotal resection; PTR, partial resection; CMT, chemotherapy; RT, radiotherapy; AT, Adjuvant Therapy; ABMSC, Autologous bone marrow stem cell transplantation; FU, follow-up.

1. Immunodeficient patients with secondary intracerebral lymphoma.
2. Patients who received lumbar puncture or experimental treatment before MR scans.
3. Patients with PCNSL located externally to the ventricle and periventricular region.

2.2. Imaging analysis

Two experienced and senior imaging diagnostic physicians independently analyzed the images using a double-blind method. They assessed the MR plain scan signals, enhancement mode, enhancement degree, site of occurrence, cyst degeneration and necrosis, lesion shape, number of lesions, peritumoral edema, and number of diffusion-weighted imaging (DWI) signals. In case of disagreement, a consensus was reached through discussion. The degree of peritumoral edema was classified as mild (range <1 cm), moderate (1–2 cm), or severe (>2 cm). The MRI plain scan signal was compared with the gray matter signal of the same layer. The apparent diffusion coefficient (ADC) of the lesions was measured using DWI data at a GE MRI post-processing workstation ADW 4.5. The rADC value was utilized to determine if diffusion was limited and whether the ADC value was high or low. 1H-MRS was employed to observe the metabolite peaks in the lesion.

2.3. Statistical analysis

The collected data were statistically analyzed using SPSS 26.0 statistical software. The measurement data were expressed as mean ± standard deviation ($\bar{x} \pm s$), and the count data were expressed as rates.

3. Results

3.1. Clinical manifestations

The enrolled patients presented with a range of symptoms, including headache, dizziness, limb weakness, memory loss, cognitive impairment, and other manifestations. One patient experienced convulsions, two had memory loss, and six exhibited limb weakness. The duration of symptom onset varied from a few days to a month (Table 1).

3.2. Imaging feature

All 13 patients underwent both plain and contrast-enhanced MR scans, and one patient also underwent an MRS examination. Among the cases, 11 showed hypointense signals and two exhibited isointense signals on T1 and T2 weighted sequences. Eight cases presented with nodules/masses, of which three were irregular in shape and two were butterfly-shaped. Mild edema was observed in nine cases, moderate edema in three cases, and severe edema in one case. All 13 cases exhibited uniform and prominent enhancement, including irregular enhancement in four cases, mass enhancement in three cases, nodular enhancement in four cases, and sphenowing enhancement in two cases. Multiple lesions were observed in eight cases, and six cases showed invasive changes in the corpus

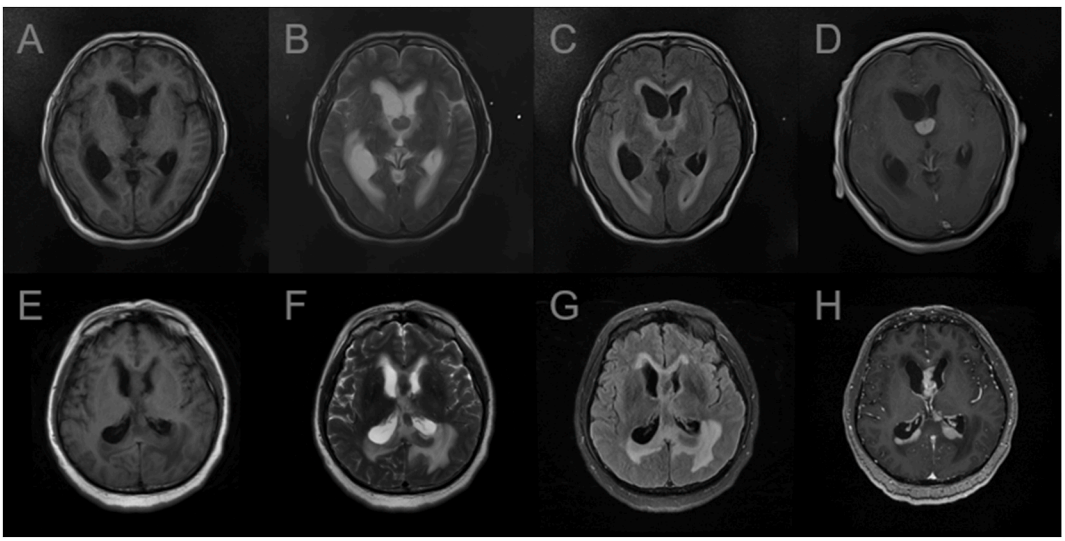

Fig. 1. A–D: Case 7, MRI plain scan shows a space-occupying lesion in the third ventricle with a slightly low signal on T1WI and focal hyperintensity on T2WI and FLAIR, while contrast-enhanced scan shows uniform enhancement. E–H: Case 11, MRI plain scan shows space-occupying lesions in both lateral and third ventricles with low signals on T1WI and focal hyperintensity on T2WI and FLAIR, while contrast-enhanced scan shows nodular, clump enhancement.

callosum. In one case, three lesions were located in different areas of the ventricle. Five cases had single lesions, with three in the lateral ventricle, one in the third ventricle, and one in the fourth ventricle. The DWI weighted sequence showed a high signal. A preoperative 1H-MRS examination of one patient revealed a decrease in the NAA peak, an increase in the Cho peak, and LL double peaks (Lac peak, Lip peak) (Fig. 1 (A-H)).

3.3. Cerebrospinal fluid features

Cerebrospinal fluid (CSF) examinations showed slightly elevated white blood cell (WBC) count and protein levels. See Table 2 for details.

3.4. Pathology and immunohistochemistry

All 13 patients were diagnosed with diffuse large B-cell lymphoma (DLBCL), characterized by neoplastic large B lymphoid cells exhibiting a diffuse growth pattern. The tumors were mainly located in the ventricle, spreading on the surface of the meninges. Five cases originated from the non-germinal center, while five cases were of germinal center origin. Immunohistochemical data were available for nine cases performed in our hospital. Epstein-Barr virus-encoded small RNA (EBER) was negative in four patients. Two cases showed MYC and Bcl-2 double-expression, including one case positive for CD5. Immunohistochemistry analysis of the nine cases demonstrated high expression of Ki-67 (70–95%), with four cases showing Ki-67 levels above 90%, indicating hyperactive proliferation of tumor cells. CD20 and MUM-1 were positive in six cases. B-cell lymphoma 2 (BCL-2) was positive in four cases and negative in four cases. BCL-6 was positive (>30%) in eight out of the nine cases. In six cases, the glial fibrillary acidic protein (GFAP) was negative, indicating residual normal brain tissue (Fig. 2 (A-D)).

3.5. Treatment

Among the 13 subjects, seven patients underwent surgical treatment followed by chemotherapy, with six of them also receiving radiotherapy. 7 out of the 13 patients underwent chemotherapy. 2 patients were administered the CTOP regimen, which consisted of epirubicin (40 mg on day 1–2), cyclophosphamide (800 mg on day 1), vindesine (4 mg on day 1) and hydroprednisone (60 mg from day 1 to day 7) by intravenous infusion, One of them underwent concurrent chemotherapy by intravenous drop with the VP-high does-methotrexate (VP-HD-MTX) regimen, which included vindesine at a dose of 4 mg on day 1, MTX at a dose of 5g on day 1, and hydroprednisone at a dose of 60 mg from day 1 to day 7 and VP + medium dose MTX therapy consisting of vindesine at a dose of 4 mg on day 1, MTX at a dose of 3g on day 1, and hydroprednisone at a dose of 60 mg from day 1 to day 7. The patient also received MTX therapy comprising cytarabine at a dose of 50 mg, methotrexate at a dose of 10 mg, and dexamethasone at a dose of 5 mg in the way of intrathecal injection. 2 patients underwent treatment with HD-MTX in combination with temozolomide: methotrexate at a dose of 5g on day 1, temozolomide at a dose of 50 mg twice daily from day 1 to day 7; methotrexate chemotherapy alone, MA regimen mobilization (cytarabine 3g twice daily day 1–2, mithoquinone 15 mg on day 1, 10 mg on day 2) and Hyper-CVAD B segment (methotrexate 2g on day 1, cytarabine 1.5g twice daily on day 2–3) were inserted into the chemotherapy regimen described above. 1 patient underwent 6 cycles of the R2-MT regimen, which consisted of rituximab at a dose of 700mgon day 0; methotrexate at a dose of 4.5g, administered on day 1; temozolomide at a dose of 200 mg, administered from day 2 to day 6; and lenalidomide at a dose of 25 mg from day 1 to day 14. The above treatments were administered intravenously. 2 patients received intravenous rituximab 660 mg on day 0, methotrexate 5.8g on day 1, and oral temozolomide 50 mg twice daily from day 1 to day 7. Lumbar puncture was performed simultaneously, and an intrathecal injection of rituximab at a dose of 40 mg was administered.

Four patients received surgical treatment alone. Case 11 and case 12 received chemotherapy without surgical resection, and case 11 also underwent autologous bone marrow stem cell transplantation.

Table 2
Cerebrospinal fluid features of the enrolled patients.

	Number of cells	Glucose (mmol/L)	Chlorides (mmol/L)	Protein (g/L)
1	22	2.98	119.2	0.74
2	–			
3	43	3.1	123.6	1.28
4	2	3.43	118.3	0.2
5	53	3.39	114.3	0.5
6	–			
7	7	4	116.3	0.64
8	43	2.68	120.8	1.043
9	–			
10	–			
11	–			
12	18	3.55	118.4	0.8
13	–			

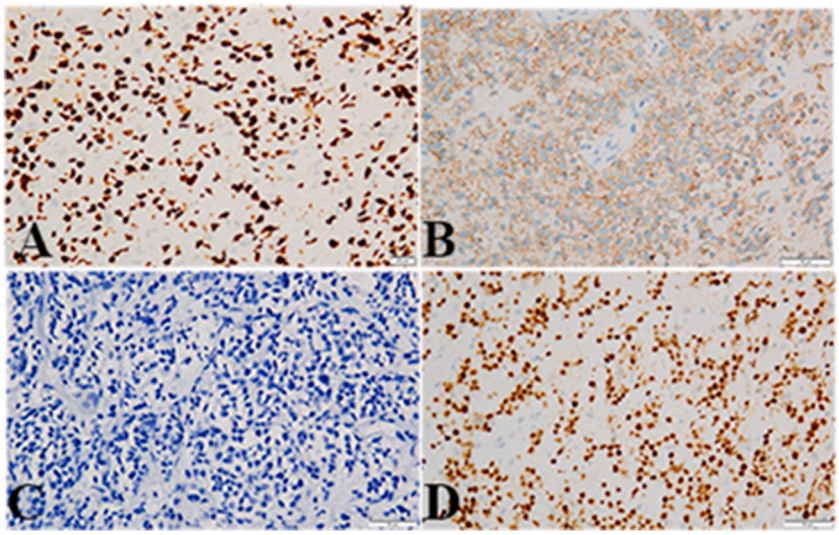

Fig. 2. Immunohistochemical results of Case 13 Tumor cells:400 × magnification, PAX-5(+) (A), CD20(+) (B), EBER(−) (C), Ki67(+) (D).

3.6. Follow-up and prognosis

During follow-up, among the 13 patients included in this study, recurrence was observed in 4 patients, with 3 lesions located in the lateral ventricle and 1 lesion located in the fourth ventricle, indicating a potential dissemination of cerebrospinal fluid. The survival time of the patients ranged from 1 month to 5 years. At the time of reporting this study, cases 11 and 13 were still alive. The mean survival time during follow-up was 23.52 months.

4. Discussion

In this study, the median age of onset for PIL cases was 57 years, with a male-to-female ratio of nine to four. The most common clinical features observed in patients were headache, dizziness, limb weakness, and memory loss. Additionally, some patients exhibited edema around the lesion and hydrocephalus caused by CSF circulation obstruction. On imaging, hypointense signals were seen on T1WI and T2WI in 11 cases. Contrast-enhanced imaging revealed uniform and prominent enhancement in all 13 cases. Multiple lesions were observed in seven cases, while single lesions were found in six cases. The lateral ventricles were the most common site of PIL, followed by the third and fourth ventricles. Pathological examination confirmed diffuse large B-cell lymphoma (DLBCL) in all 13 cases, characterized by neoplastic large B lymphoid cells exhibiting a diffuse growth pattern. Immunohistochemical analysis showed high expression of Ki-67 in all nine cases examined. Among the 13 subjects, seven received surgical treatment followed by chemotherapy, while three received surgical treatment alone. This study provides a comprehensive overview of the epidemiology, imaging and pathological features, clinical symptoms, treatment, and prognosis of PIL through a cohort study, contributing to a better understanding of the early diagnosis and treatment of PIL.

The incidence of PCNSL is 0.44/100,000, accounting for approximately 2% of all primary CNS tumors, while PIL is even rarer [5]. The average onset age of PIL in this study was 56 years, with a median age of 57 years (ranging from 39 to 70 years), consistent with previous reports [9]. The male-to-female ratio in this study was 9:4, indicating a higher prevalence of PIL in men, which aligns with existing literature [10].

The symptoms of PIL largely depend on the specific area of the CNS involved. Most lesions appear as nodular masses [9,11–13]. Brain MRI typically shows iso- or hyperintense signals on T1WI and T2WI, with significant homogeneous enhancement on contrast-enhanced scans. Unlike PCNSL in the brain parenchyma, PIL often exhibits irregular morphology and shows a creeping growth pattern along the ventricular wall and choroid plexus. Lesions located in the fourth ventricle can extend outward along the foramen of the fourth ventricle [4]. There have also been reports of PIL with diffuse involvement of the fourth ventricle and hypothalamus [14]. Due to the characteristics of tumor cells, such as reduced cytoplasm, large nuclei, tightly arranged cells, limited extracellular space, and restricted diffusion of water molecules, DWI typically shows a high signal, while ADC shows a low signal [15]. MRS can provide information on metabolic changes in the lesion tissue [15]. Susceptibility-weighted imaging (SWI) can reveal veins and hemorrhage within the tumor [16]. 18-fluorodeoxyglucose (FDG) or 11C-methionine positron emission tomography (PET) are useful for diagnosis and differential diagnosis and have the potential to predict treatment response at early stages. These advanced imaging techniques may ultimately offer non-invasive imaging biomarkers that identify high-risk PCNSL patients with poor prognoses, facilitating personalized treatment planning.

Approximately 90% of PCNSL cases are classified as diffuse large B-cell lymphoma (DLBCL), a distinct subtype according to the World Health Organization (WHO) classification [17]. DLBCL cases in the CNS frequently exhibit positive Melanoma-associated

antigen (MUM1)/interferon regulatory factor 4 (IRF4) expression, while B-cell chronic lymphocytic leukemia (CLL)/lymphoma 6 (BCL-6) is expressed in approximately 50% of cases. B-cell CLL/lymphoma 2 (BCL-2) expression varies, and CD10 is only found in a small percentage (around 10%) of cases [18,19]. Therefore, the majority of PCNS DLBCL cases resemble the post-germinal center or activated B-cell (ABC) immunophenotype ($CD10^{-}$, BCL6+, MUM1/IRF4+). BCL-6, CD10, BCL-2, MUM1/IRF4, and Ki-67 are important indicators for assessing prognosis. Recent studies suggest that BCL-6 expression is associated with poor survival outcomes among B-cell differentiation markers [20].

Currently, the treatment of PIL is based on the treatment principles for PCNSL. Due to the diffuse infiltration and deep location of PIL, surgical treatment may not only fail to prolong patient survival but also cause severe damage to the nervous system. However, surgical intervention may be considered for localized lesions, particularly in cases with acute obstructive hydrocephalus. Chemotherapy has become the first-line treatment for PCNSL. The choice of chemotherapy drugs is crucial due to the blood-brain barrier, which affects drug effectiveness. Methotrexate (MTX) at a dose of 3.5g/m2 is recommended as the standard therapeutic dose, as it demonstrates good efficacy and safety. Higher doses of MTX do not provide additional benefits [21]. Most studies on systemic chemotherapy for PCNSL advocate for combining high-dose MTX with other chemotherapy drugs to improve patient survival rates, with high-dose cytarabine (HD-Ara-C) being the most commonly used drug in combination. Ferreri et al. [22] have shown that MTX combined with Ara-C is superior to MTX chemotherapy alone. Temozolomide, an imidazole-tetrazine alkylating agent that can cross the blood-brain barrier [23], is suitable for elderly patients due to its low toxicity and high safety. Intrathecal chemotherapy with MTX, Ara-C, and dexamethasone is commonly used in combination with intravenous chemotherapy. Studies have demonstrated that high-dose MTX-based intravenous chemotherapy combined with intrathecal MTX injection or intrathecal MTX alone can effectively treat PCNSL with meningeal involvement, but further randomized controlled clinical trials are needed for validation [24,25]. Birnbaum et al. [26] have suggested that the addition of rituximab significantly improves the clinical efficacy of chemotherapy. High-dose chemotherapy with autologous stem cell transplantation (HDC + ASCT) enhances the bioavailability of drugs and achieves better therapeutic effects through high-dose chemotherapy supported by hematopoietic stem cells [27]. HDC-ASCT can be considered for patients with newly diagnosed or relapsed/refractory PCNSL, particularly in younger patients (age <65 years old) [25,28].

In this study, 11 patients died, and four patients experienced a relapse. PIL is a rare disease, and its clinical symptoms are often nonspecific, primarily manifested as increased intracranial pressure. Key imaging features include cluster growth along the choroid plexus and diffuse growth along the ventricular wall. Surgical resection is a viable option for localized lesions, particularly in patients with significant tumor mass effects or acute obstructive hydrocephalus. Radiotherapy and chemotherapy are commonly used and necessary treatment modalities. This retrospective study provides a comprehensive understanding of common clinical features and unique imaging findings of patients with PIL. We found that PIL patients had specific imaging characteristics such as hypointense signals on MRI, nodules/masses with varying shapes, and prominent enhancement.

5. Conclusions

The study focused on primary intraventricular lymphoma (PIL), a rare subtype of primary central nervous system lymphoma (PCNSL), accounting for 4.4%–11.8% of PCNSL cases. The research aimed to describe clinical and imaging findings in a cohort of 13 patients with PIL, confirming diagnoses through surgery and pathology. The patients, predominantly males with a mean age of 56 years, presented with varied symptoms such as headache, limb weakness, and cognitive impairment. Imaging analysis revealed hypointense signals on MRI, nodules/masses with varying shapes, and prominent enhancement. Pathologically, all cases were diffuse large B-cell lymphoma (DLBCL) with high Ki-67 expression. Treatment approaches varied, with some patients undergoing surgery followed by chemotherapy and radiotherapy. The study's findings underscore the complexity of PIL diagnosis and treatment, emphasizing the need for further research to optimize therapeutic strategies and improve patient outcomes in this challenging condition.

Ethics approval and consent to participate

The study was approved by the Ethics Committee of the Affiliated Hospital of Xuzhou Medical University. We confirm that all methods were performed in accordance with the ethical standards as laid down in the Declaration of Helsinki and its later amendments or comparable ethical standards.

Consent for publication

Not applicable.

Availability of data and materials

The data will be available on request to the corresponding author.

Funding

This study was funded by Open subject of provincial key laboratories of universities in Jiangsu Province (XZSYSKF2020010), Xuzhou Municipal Health Commission's 2020 Youth Medical Science and Technology Innovation Project (key project) (XWKYHT20200001), and the 2020 Xuzhou Medical University Affiliated Hospital Science and Technology Development Fund Project (key project) (XYFZ2020008).

CRediT authorship contribution statement

Yuqiao Wang: Writing – original draft, Methodology, Conceptualization. **Chengcheng Cui:** Writing – original draft, Methodology, Investigation. **Hafiz Khuram Raza:** Writing – review & editing, Methodology. **Hao Chen:** Writing – review & editing, Methodology. **Xiangbu Wang:** Methodology, Investigation, Data curation. **Wei Zhang:** Investigation, Data curation. **Wenqing Meng:** Formal analysis, Data curation. **Keke Li:** Methodology, Investigation. **Zhifeng Mao:** Writing – review & editing. **Xiujuan Sun:** Writing – review & editing. **Shenyang Zhang:** Supervision, Data curation, Conceptualization.

Declaration of competing interest

The authors declare that they have no known competing financial interests or personal relationships that could have appeared to influence the work reported in this paper.

Acknowledgements

None.

References

[1] A. Basavaraj, M. Kadam, D. Kadam, Primary Maxillary Sinus Plasmablastic lymphoma in HIV/AIDS, J. Assoc. Phys. India 64 (5) (2016) 71–72.
[2] T. Sugino, T. Mikami, Y. Akiyama, M. Wanibuchi, T. Hasegawa, N. Mikuni, Primary central nervous system anaplastic large-cell lymphoma mimicking lymphomatosis cerebri, Brain Tumor Pathol. 30 (1) (2013) 61–65.
[3] W. Küker, T. Nägele, A. Korfel, S. Heckl, E. Thiel, M. Bamberg, M. Weller, U. Herrlinger, Primary central nervous system lymphomas (PCNSL): MRI features at presentation in 100 patients, Journal of neuro-oncology 72 (2) (2005) 169–177.
[4] L. Cheng, H. Zhu, J. Wang, G. Wang, X. Ma, K. Zhao, J. Wang, K. Shu, Clinical features, diagnosis, and treatment of primary intraventricular lymphoma: insights from a monocentric case series, Front. Neurol. 13 (2022) 920505.
[5] Q. Ostrom, H. Gittleman, J. Fulop, M. Liu, R. Blanda, C. Kromer, Y. Wolinsky, C. Kruchko, J. Barnholtz-Sloan, CBTRUS Statistical Report: Primary Brain and Central Nervous System Tumors Diagnosed in the United States in 2008-2012, 2015. Neuro-oncology.iv1-iv62.
[6] G. Cheng, J. Zhang, Imaging features (CT, MRI, MRS, and PET/CT) of primary central nervous system lymphoma in immunocompetent patients, Neurol. Sci. : official journal of the Italian Neurological Society and of the Italian Society of Clinical Neurophysiology 40 (3) (2019) 535–542.
[7] L. von Baumgarten, G. Illerhaus, A. Korfel, U. Schlegel, M. Deckert, M. Dreyling, The diagnosis and treatment of primary CNS lymphoma, Dtsch Arztebl International 115 (25) (2018) 419–426.
[8] T. Chen, Y. Liu, Y. Wang, Q. Chang, J. Wu, Z. Wang, D. Geng, J.-T. Yu, Y. Li, X.-Q. Li, et al., Evidence-based expert consensus on the management of primary central nervous system lymphoma in China, J. Hematol. Oncol. 15 (1) (2022) 136.
[9] Y. Zhu, K. Ye, R. Zhan, Y. Tong, Multifocal lateral and fourth ventricular primary central nervous system lymphoma: case report and literature review, Turkish neurosurgery 25 (3) (2015) 493–495.
[10] J. Mendez, Q. Ostrom, H. Gittleman, C. Kruchko, L. DeAngelis, J. Barnholtz-Sloan, C. Grommes, The elderly left behind-changes in survival trends of primary central nervous system lymphoma over the past 4 decades, Neuro Oncol. 20 (5) (2018) 687–694.
[11] R. Brar, A. Prasad, T. Sharma, N. Vermani, Multifocal lateral and fourth ventricular B-cell primary CNS lymphoma, Clin. Neurol. Neurosurg. 114 (3) (2012) 281–283.
[12] V. Suri, V. Mittapalli, M. Kulshrestha, K. Premlani, S. Sogani, K. Suri, Primary intraventricular central nervous system lymphoma in an immunocompetent patient, J. Pediatr. Neurosci. 10 (4) (2015) 393–395.
[13] G. Khanna, S. Ahlawat, N. Garg, R. Gupta, R. Patir, A rare case of isolated intraventricular primary central nervous system lymphoma in an 85-year-old man, Asian journal of neurosurgery 16 (3) (2021) 623–625.
[14] M. Cellina, V. Fetoni, P. Baron, M. Orsi, G. Oliva, Unusual primary central nervous system lymphoma location involving the fourth ventricle and hypothalamus, NeuroRadiol. J. 28 (2) (2015) 120–125.
[15] R. Barajas, J. Rubenstein, J. Chang, J. Hwang, S. Cha, Diffusion-weighted MR imaging derived apparent diffusion coefficient is predictive of clinical outcome in primary central nervous system lymphoma, AJNR American journal of neuroradiology 31 (1) (2010) 60–66.
[16] S. Peters, N. Knöß, F. Wodarg, C. Cnyrim, O. Jansen, Glioblastomas vs. lymphomas: more diagnostic certainty by using susceptibility-weighted imaging (SWI), RoFo : Fortschritte dem Geb. Rontgenstrahlen Nukl. 184 (8) (2012) 713–718.
[17] M. Miwa, H. Tokuda, K. Tsushita, J. Kotoyori, Y. Takahashi, N. Ozaki, O. Kozawa, Y. Oiso, Involvement of pertussis toxin-sensitive GTP-binding protein in prostaglandin F2 alpha- induced phosphoinositide hydrolysis in osteoblast-like cells, Biochem. Biophys. Res. Commun. 171 (3) (1990) 1229–1235.
[18] C. Giannini, A. Dogan, D. Salomão, CNS lymphoma: a practical diagnostic approach, J. Neuropathol. Exp. Neurol. 73 (6) (2014) 478–494.
[19] H. Yano, Y. Fujiwara, Y. Komohara, Cholesterol metabolism and lipid droplet vacuoles; a potential target for the therapy of aggressive lymphoma, J. Clin. Exp. Hematop. : JCEH 62 (4) (2022) 190–194.
[20] S. Kreher, K. Jöhrens, F. Strehlow, P. Martus, K. Borowiec, J. Radke, F. Heppner, P. Roth, E. Thiel, T. Pietsch, et al., Prognostic impact of B-cell lymphoma 6 in primary CNS lymphoma, Neuro Oncol. 17 (7) (2015) 1016–1021.
[21] L. Schaff, C. Grommes, Updates on primary central nervous system lymphoma, Curr. Oncol. Rep. 20 (2) (2018) 11.
[22] A. Ferreri, M. Reni, M. Foppoli, M. Martelli, G. Pangalis, M. Frezzato, M. Cabras, A. Fabbri, G. Corazzelli, F. Ilariucci, et al., High-dose cytarabine plus high-dose methotrexate versus high-dose methotrexate alone in patients with primary CNS lymphoma: a randomised phase 2 trial, Lancet (London, England) 374 (9700) (2009) 1512–1520.
[23] G. Xu, M. Yang, H. Tong, L. Mao, J. Jin, High-dose methotrexate plus temozolomide as a salvage treatment in metastatic central nervous system Lymphoma: two cases report and review of literature, Int. J. Clin. Exp. Med. 8 (5) (2015) 8222–8225.
[24] G. Citterio, M. Reni, A. Ferreri, Present and future treatment options for primary CNS lymphoma, Expet Opin. Pharmacother. 16 (17) (2015) 2569–2579.

[25] K. Hoang-Xuan, E. Bessell, J. Bromberg, A. Hottinger, M. Preusser, R. Rudà, U. Schlegel, T. Siegal, C. Soussain, U. Abacioglu, et al., Diagnosis and treatment of primary CNS lymphoma in immunocompetent patients: guidelines from the European Association for Neuro-Oncology, Lancet Oncol. 16 (7) (2015) e322–e332.
[26] T. Birnbaum, E. Stadler, L. von Baumgarten, A. Straube, Rituximab significantly improves complete response rate in patients with primary CNS lymphoma, Journal of neuro-oncology 109 (2) (2012) 285–291.
[27] A. Omuro, D. Correa, L. DeAngelis, C. Moskowitz, M. Matasar, T. Kaley, I. Gavrilovic, C. Nolan, E. Pentsova, C. Grommes, et al., R-MPV followed by high-dose chemotherapy with TBC and autologous stem-cell transplant for newly diagnosed primary CNS lymphoma, Blood 125 (9) (2015) 1403–1410.
[28] N. Alimohamed, A. Daly, C. Owen, P. Duggan, D. Stewart, Upfront thiotepa, busulfan, cyclophosphamide, and autologous stem cell transplantation for primary CNS lymphoma: a single centre experience, Leuk. Lymphoma 53 (5) (2012) 862–867.